KSME Journal, Vol. 7, No. 3, pp. 282~289, 1993

An Effectiveness-NTU Method for Triple-Passage Counterflow Heat Exchangers

Yun-Ho Cho and Ho-Myung Chang*

(Received March 11, 1993)

A new effectiveness-NTU method is developed for a special type of heat exchangers, in which the fluid of a passage is in simultaneous thermal contact with two separate fluids flowing in the opposite direction. An extensive amount of numerical simulations are carried out by an iterative method for wide ranges of dimensionless parameters such as ratios of capacity rates, NTU's, or a dimensionless inlet temperature. The large body of resulting data are then effectively reduced to a small number of simple equations and graphs by introducing a new effectiveness, ε. ε is defined as the ratio of actual heat transfer to the maximum heat transfer obtained when the NTU's become very large while the ratio of two NTU's is kept constant. The developed method is readily applicable to the cycle analysis and design, in the same way as the ε-NTU method for the usual double-passage heat exchangers.

Key Words: Heat Exchanger, Triple-Passage, Counterflow Heat Exchanger, Heat Exchanger Effectiveness, Number of Transfer Unit (NTU)

Nomenclature

A : Heat exchange area, m^2
C : Flow-stream capacity rate, kW/K =(mass flow rate)×(specific heat at constant pressure)
g : Coefficient of function $G(X)$, dimensionless
G : Funciton of X, defined by Eq. (21), dimensionless
L : Heat exchanger length, m
N : Ratio of two NTU's, defined by Eq. (18)
NTU : Number of transfer unit, dimensionless
q : Heat transfer rate, kW
T : Fluid temperature, K
U : Overall heat transfer coefficient, kW/m^2-K
x : Axial flow coordinate, m
X : Parameter related to fluid capacity rates, defined by Eq. (14)

Geek Letter Symbols

ε : Heat exchanger effectiveness, dimensionless
θ : Dimensionless temperature
ξ : Dimensionless axial flow coordinate

Subscript

1 : Hot fluid with higher inlet temperature
2 : Hot fluid with lower inlet temperature
3 : Cold fluid
max : Maximum value
min : Minimum value

* Department of Mechanical Engineering, Hong Ik University, Seoul 121-791, Korea

1. Introduction

Triple-passage counterflow heat exchangers are frequently encountered in recent design processes of low temperature refrigeration and liquefaction systems. The heat exchangers are used so that the fluid of a passage exchanges heat simultaneously with two separate fluids flowing in the opposite direction. Figure 1 shows a schematic representation of fluid temperature distributions for a case when a cold fluid, 3, is in thermal

contact with two hot fluids, 1 and 2. Two simple geometric configurations for the heat exchangers are shown in Fig. 2. It is noted that the fluids 1 and 2 are not in direct thermal contact. In real applications, the inner tubes have fins on their outer surfaces in order to increase the heat transfer areas.

Application areas of the triple-passage counterflow heat exchangers are described in many recent publications. A typical application is the liquefaction plant for cryogenic gases, such as helium or hydrogen. Ganni, Moor and Winn(1986) reported that an existing plant was modified by employing the triple-passage heat exchangers to upgrade the liquefying capacity and efficiency.

Applications of the heat exchangers are significantly extended by a practical usage of superconducting magnets. For a reliable and economic operation of the magnet systems, a continuous refrigeration at liquid helium temperature (4.2 K) becomes increasingly important. Depending on the sizes of the magnet systems, the various sizes

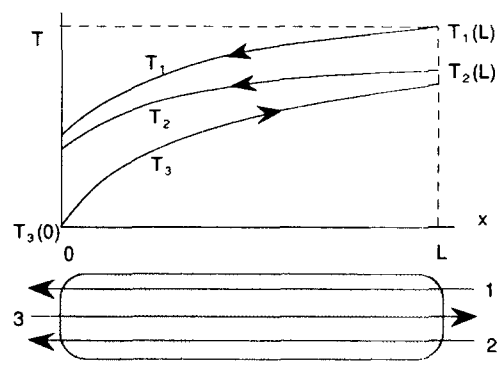

Fig. 1 Schematic temperature distributions of three fluids in a triple-passage counterflow heat exchanger

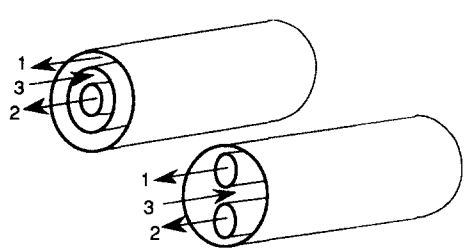

Fig. 2 Two simplest configurations of triple-passage counterflow heat exchangers

of refrigerators are under active development. It does not seem to be coincidental that many of the refrigeration systems should have the triple-passage heat exchangers as components. One of the reasons might be that new turboexpanders are replacing classical reciprocating expanders to extract work from the refrigerant (Timmerhaus and Flynn, 1989). Since the pressure ratio should be smaller with the turboexpanders, refrigeration is obtained through multi-expansion and the triple-passage heat exchangers are necessary in between the stages. Figure 3 shows schematically one of the typical refrigeration cycles for liquid helium temperature with two turboexpanders and a triple-passage counterflow heat exchanger.

Some examples of large scale applications of the heat exchangers are the refrigeration systems for the fusion reactors (Slack, Nelson and Chronis, 1986 ; Yamamoto et al., 1990), the colliders (Dauvergne, Firth and Juillerat, 1990 ; Tsuchiya et al., 1990 ; Tsuchiya et al., 1992), and accelerators (Brindza, Chronis and Rode, 1988). The refrigeration systems for the superconducting generators (Yanagi et al., 1992 ; Asakura et al. 1992) also have the heat exchangers as their components. Magnetic resonance devices with the superconducting magnets, such as magnetic resonance imaging (Clausen et al., 1990) and magnetic resonance spectroscopy (Aoki et al., 1992), require the refrigeration for which the combination of small turboexpanders and a triple-passage heat exchanger is to be used. More recently, thermodynamic cycle analysis was performed for various cycle configurations with triple-or multiple-passage heat exchangers (Ziegler and Quack, 1992).

In spite of the significant usage of the triple-passage heat exchangers, any accurate information on the heat exchange characteristics is not available. Moreover, the simple heat exchange relation of ε-NTU method (Kays and London, 1984) for the conventional two-passage heat exchangers cannot be easily modified for the triple-passage heat exchangers. The reasons are that the number of the parameters involved is much greater and that one of the fluids interacts simultaneously with other two fluids.

This work is proposed to derive a simple and useful heat exchange relation for the triple-passage heat exchangers. The results should be applicable to the cycle analysis and design of the refrigeration systems, just like the ε-NTU method for the usual double-passage heat exchangers. This paper describes briefly the formulation and the solution procedure of the problem, and presents a new ε-NTU method that is obtained from results of numerical calculation.

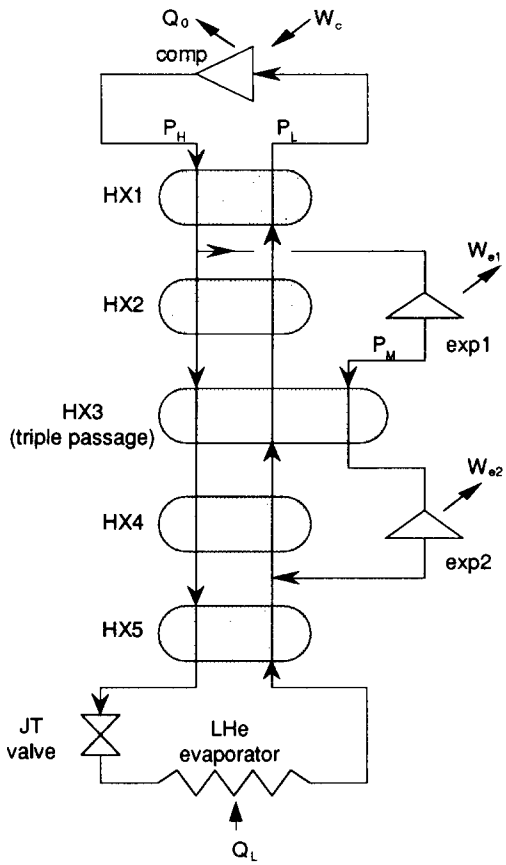

Fig. 3 Schematic of refrigeration cycle for liquid helium temperature with two turboexpanders and a triple-passage counterflow heat exchanger

P_H : high pressure
P_L : low pressure
P_M : intermediate pressure
W_c : compression work-in
Q_0 : Heat rejected at room temperature
Q_L : refrigeration or heat absorbed at low temperature
W_{e1}, W_{e2} : expansion work-out, 1 and 2

2. Formulation of Problem

2.1 Governing equations

Steady energy balance equations can be written for the three fluids as

$$C_1\frac{dT_1}{dx}=U_{13}(T_1-T_3)\frac{A_{13}}{L}, \tag{1}$$

$$C_2\frac{dT_2}{dx}=U_{23}(T_2-T_3)\frac{A_{23}}{L}, \tag{2}$$

$$C_3\frac{dT_3}{dx}=-U_{13}(T_3-T_1)\frac{A_{13}}{L}-U_{23}(T_3-T_2)\frac{A_{23}}{L}, \tag{3}$$

when the fluid properties, heat transfer coefficients and heat exchange areas per unit length are constant along the flow direction, and the axial thermal diffusion can be neglected. In Eqs. (1), (2), and (3), the axial flow coordinate, x, is selected from the inlet point of the fluid, 3, flowing against two other fluids. Out of the two fluids fluids flowing in the same direction, the fluid of the higher inlet temperature is denoted by 1. Boundary conditions of the differential equations are the three inlet temperatures,

$$T_1(L),\ T_2(L),\ T_3(0)$$

Generally, the three solutions, $T_1(x)$, $T_2(x)$, $T_3(x)$, are functions of x. Of special interest are the three exit temperatures, $T_1(0)$, $T_2(0)$, $T_3(L)$, and the total heat transfer rate for fluid 3,

$$q_3=C_3\{T_3(L)-T_3(0)\}=C_1\{T_1(L)-T_1(0)\}+C_2\{T_2(L)-T_2(0)\} \tag{4}$$

The second equality of Eq. (4) can be derived simply by combining and integrating Eqs. (1), (2) and (3).

2.2 Dimensionless parameters

By using dimensionless variables and parameters,

$$\theta(\xi)=\frac{T(x)-T_3(0)}{T_1(L)-T_3(0)},\quad \xi=\frac{x}{L},$$

$$NTU_1=\frac{(UA)_{13}}{C_1},\quad NTU_2=\frac{(UA)_{23}}{C_2}, \tag{5}$$

the governig equations and the boundary conditions can be nondimensionalized as follows.

$$\frac{d\theta_1}{d\xi}=NTU_1(\theta_1-\theta_3), \tag{6}$$

$$\frac{d\theta_2}{d\xi}=NTU_2(\theta_2-\theta_3), \tag{7}$$

$$\frac{d\theta_3}{d\xi}=-\frac{C_1}{C_3}NTU_1(\theta_3-\theta_1) -\frac{C_2}{C_3}NTU_2(\theta_3-\theta_2), \tag{8}$$

$$\theta_1(1)=1,\ \theta_2(1)=\text{given},\ \theta_3(0)=0 \tag{9}$$

It is noted that dimensionless temperature, θ, should have a range between 0 and 1 and that the definitions of two NTU's are consistent with the conventional Number of Transfer Unit insofar as $C_1\leq C_3$ and $C_2\leq C_3$. When Eqs. (6) to (8) are solved, the dimensionless exit temperatures become functions of five dimensionless parameters

$$\theta_1(0),\theta_2(0),\theta_3(1)=\text{fns}\left(NTU_1, NTU_2, \frac{C_1}{C_3}, \frac{C_2}{C_3}, \theta_2(1)\right) \tag{10}$$

The three exit temperatures are related by the dimensionless form of the energy balance, Eq. (4),

$$\theta_3(1)=\frac{C_1}{C_3}\{1-\theta_1(0)\}+\frac{C_2}{C_3}\{\theta_2(1)-\theta_2(0)\} \tag{11}$$

3. Numerical Method

The system of differential equations, Eqs. (6), (7) and (8) are solved numerically for various values of the five input parameters. Fourth order Runge-Kutta method is used to integrate the differential equations. Since the three boundary conditions are not given at one point, the solution method should be an iterative one.

The integration starts from $\xi=1$ with the given initial conditions of $\theta_1(1)=1$ and $\theta_2(1)$, and with a gauss of $\theta_3(1)$. When the integration reaches $\xi=0$, $\theta_3(0)$ should be 0. If $\theta_3(0)$ is not equal to 0, integration is repeated with a new guess of $\theta_3(1)$ value. This process is repeated until the calculated $\theta_3(0)$ equals 0.

The number of steps for a calculation was 1,000 so that the numerical stability could be maintained for a steep change of temperatures for large NTU's. The computation was stopped when the absolute value of $\theta_3(0)$ is less than 10^{-6}. When the next guess of $\theta_3(1)$ value was determined by a linear interpolation of two previous computation results, the solution was obtained within several iterations for most cases.

4. Results and Discussion

For various values of the five input parameters in Eq. (10), sets of three exit temperatures were obtained. After examining the data sets, a new ε-NTU method for evaluating the exit conditions was suggested. The basic idea of the method is that the three exit temperatures are expressed in terms of only one effectiveness for the triple-passage counterflow heat exchangers.

4.1 Definition of effectiveness

Effectiveness of the triple-passage counterflow heat exchangers is defined as the ratio of the actual heat transfer of fluid 3 to the maximum heat transfer obtained for very large values of NTU's with the ratio of the NTU's kept constant. In dimensionless form, the effectiveness is simply the ratio of $\theta_3(1)$ to maximum $\theta_3(1)$.

$$\varepsilon\equiv\frac{q_3}{q_{3,\max}}=\frac{\theta_3(1)}{(\theta_3(1))_{\max}} \tag{12}$$

It should be noted that the maximum value of $\theta_3(1)$ is a function of only four parameters.

$$(\theta_3(1))_{\max}=\text{fn}\left(\frac{NTU_1}{NTU_2}, \frac{C_1}{C_3}, \frac{C_2}{C_3}, \theta_2(1)\right) \tag{13}$$

4.2 Maximum heat transfer

The maximum $\theta_3(1)$ is to be considered as a dimensionless measure of the maximum heat transfer. It was found that the maximum value can be expressed as a relatively simple function of the dimensionless parameter. The expressions are presented with two different sets of functions, depending upon the sum of two capacity ratios, denoted by X.

$$X\equiv\frac{C_1}{C_3}+\frac{C_2}{C_3}=\frac{C_1+C_2}{C_3} \tag{14}$$

Two different domains for the expressions can be explained in $C_1/C_3-C_2/C_3$ plane as shown in Fig. 4.

4.2.1 Case 1 : X≤1

In this case, the capacity rate of the fluid 3 is greater than the sum of those of the other two

fluids. It was found from the numerical data sets that both $\theta_1(0)$ and $\theta_2(0)$ reach 0 as the NTU's become large, regardless of the NTU ratio, C_1/C_3, C_2/C_3, and $\theta_2(1)$.

$$(\theta_1(0))_{min}=(\theta_2(0))_{min}=0 \tag{15}$$

As a result, the maximum heat transfer or the dimensionless exit temperature of fluid 3 becomes

$$(\theta_3(1))_{max}=\frac{C_1}{C_3}+\frac{C_2}{C_3}\theta_2(1), \tag{16}$$

from Eq. (11). The maximum $\theta_3(1)$ is independent of NTU's when compared with Eq. (13). Figure 5 shows a schematic temperature distributions of three fluids in this situation.

4.2.2 Case 2: $X\leq 1$, $C_1/C_3\leq 1$ and $C_2/C_3\leq 1$

This case is more relevant for the typical cycle analysis such as that shown in Fig. 3, because the specific heat of the gases is greater at higher pressures than at lower pressures for a given temperature. In this case, the maximum $\theta_3(1)$ is very nicely fitted in terms of the four dimensionless parameters in Eq. (13) as,

$$(\theta_3(1))_{max}=1-\left(\frac{C_2}{C_1+C_2}-0.3(X-1)\log N\right)\{1-\theta_2(1)\}, \tag{17}$$

where

$$N=\frac{NTU_1}{NTU_2} \tag{18}$$

It should be noted that when $X=1$ Eq. (17) is reduced to Eq. (16), since $C_1+C_2=C_3$. In other words, at the boundary of the two cases, the temperature can be evaluated via either Eq. (16) or Eq. (17).

Equation (17) was obtained by finding the best interpolating functions from the thousands of numerical data sets. The first step of the procedure was to prepare the large data sets in the form of Eq. (13). Next, it was immediately observed that when $N=1$, the maximum $\theta_2(1)$ could be expressed exactly as

$$(\theta_3(1))_{max}=1-\frac{C_2}{C_1+C_2}\{1-\theta_2(1)\}$$

Finally, the deviation from the maximum $\theta_3(1)$ for $N=1$ was corrected for various N's, arriving at Eq. (17).

Some physical interpretations of Eq. (17) are possible with Fig. 6. When two NTU's have the same order, the maximum exit temperature of

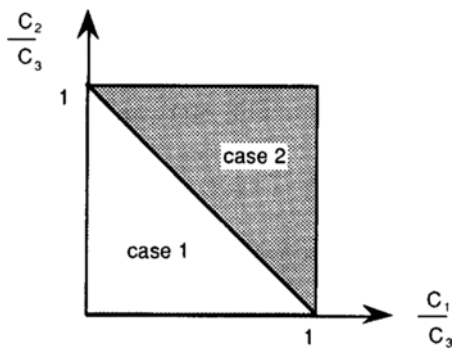

Fig. 4 Domain of case 1 and case 2 in $C_1/C_3-C_2/C_3$ plane

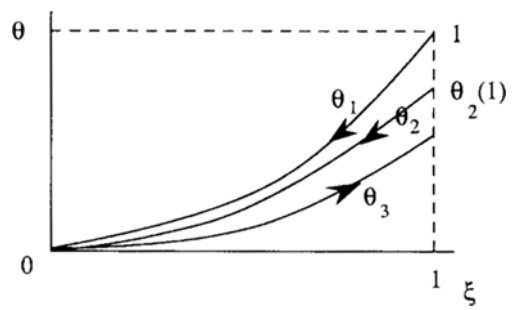

Fig. 5 Schematic temperature distributions for case 1 ($X<1$) when $\varepsilon\approx 1$

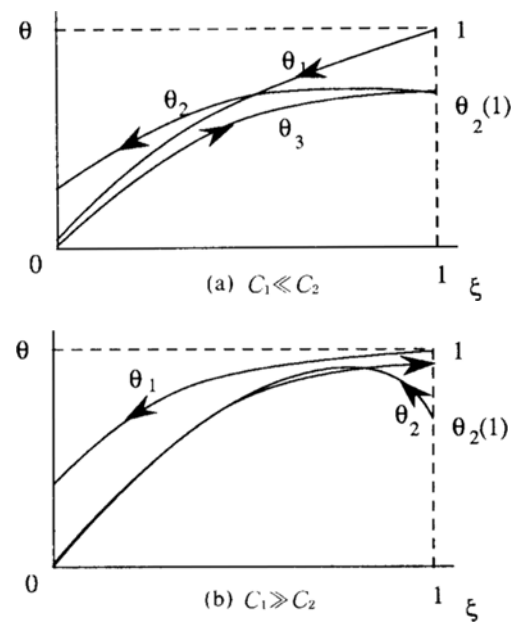

Fig. 6 Schematic temperature distributions for case 2 ($X>1$) when $\varepsilon\approx 1$

fluid 3 is determined by the two ratios of the capacity rates. In an extreme case that the capacity rate of fluid 2 is much greater than that of fluid 1, it can be simply shown from Eq. (17) that the maximum exit temperature approaches $\theta_2(1)$. In this case, the temperature distributions are similar to the case that fluids 2 and 3 exchange heat each other as shown in Fig. 6(a). In the opposite extreme case that the capacity rate of fluid 1 is much greater, the maximum exit temperature approaches 1 from Eq. (17). In this case, the distributions are similar to the case that fluids 1 and 3 exchange heat each other as shown in Fig. 6(b). An interesing behavior is that the fluid 2 is heated at its entrance region until the temperature of fluid 2 reaches the temperature of fluid 3. In general cases, the the maximum $\theta_3(1)$ may have the value between 1 and $\theta_2(1)$, depending on the two capacity rates.

The minimum temperatures of the other two fluids can be approximately expressed as

$$(\theta_1(0))_{\min}=\frac{X-1}{X}\left\{1-\left(\frac{C_2}{C_1+C_2}+0.3\log N\right)\{1-\theta_2(1)\}-\sqrt{\frac{C_2}{C_1}}\frac{C_1+C_2\theta_2(1)}{C_1+C_2}G(X)\log N\right\}, \tag{19}$$

$$(\theta_2(0))_{\min}=\frac{X-1}{X}\left\{1-\left(\frac{C_2}{C_1+C_2}+0.3\log N\right)\{1-\theta_2(1)\}+\sqrt{\frac{C_1}{C_2}}\frac{C_1+C_2\theta_2(1)}{C_1+C_2}G(X)\log N\right\}, \tag{20}$$

where

$$\begin{aligned}G(X)&=X(g_0+g_1X+g_2X^2)\\ g_0&=2.528373\\ g_1&=-2.057157\\ g_2&=0.465666,\end{aligned} \tag{21}$$

and N is defined by Eq. (18). It is noted that when $X=1$, Eq. (19) and (20) are reduced to Eq. (15). Equations (17), (19) and (20) have been checked to always satisfy Eq. (11).

Equations (19) and (20) were derived in the same way as Eq. (17). From the large data sets, it was immediately observed that when $N=1$, the minimum $\theta_1(0)$ and $\theta_2(0)$ had the same value and could be expressed exactly as

$$(\theta_1(0))_{\min}=(\theta_2(0))_{\min}=\frac{X-1}{X}\frac{C_1+C_2\theta_2(1)}{C_1+C_2}$$

$$=\frac{X-1}{X}\left[1-\frac{C_2}{C_1+C_2}\{1-\theta_2(1)\}\right]$$

The deviation from the minimum $\theta_1(0)$ and $\theta_2(0)$ for $N=1$ was corrected for various N's. Since the behavior of the two values was more complicated than that of the maximum $\theta_3(1)$, several functional expressions were possible. Among them, Eqs. (19) to (21) were determined to be the best.

These dimensionless exit temperatures for the maximum heat transfer were derived by correcting the deviation from an exactly balanced case, $N=1$, $C_1/C_3=C_2/C_3=0.5$ and $\theta_2(1)=1$. Therefore, the calculated values approach the exact values more closely as the dimensionless parameters approach the values for the balanced case. Generally speaking, the above expression is valid for every value of the parameters in the case 2 domain. On the other hand, it is most accurate, to within three decimal points, when

$$\frac{1}{2}\le\frac{C_1}{C_2}\le 2,\ \frac{1}{5}\le\frac{NTU_1}{NTU_2}\le 5,\ 0.6\le\theta_2(1)\le 1$$

4.3 Effectiveness

Usefulness of this method can be found in evaluation of the exit temperatures for finite NTU's by one effectiveness. The effectiveness, ε, is a function of the five parameters introduced in Eq. (10). While the functional expression could be found in an analytical form, the accuracy of the values derived from such an expression did not seem to be acceptable. Thus, the effectiveness was instead explicitly shown with the aid of graphs as a function of two NTU's and several values of the other three parameters.

Figure 7 through Fig. 10 were generated only for a few values of the three parameters, due to the space limitations (for details, see Chang et al., 1993). If desired, graphs for more values of the parameters may be added, and the effectiveness for most of real cases could be interpolated from the generated graphs to a satisfactory accuaracy.

Once the effectiveness is found for the given conditions, the exit temperature $\theta_3(1)$ is immediately calculated from the corresponding maximum temperatures and Eq. (12). The other two exit temperatures, $\theta_1(0)$ and $\theta_2(0)$ are obtained with the effectiveness and the corresponding minimum temperatures, approximately by

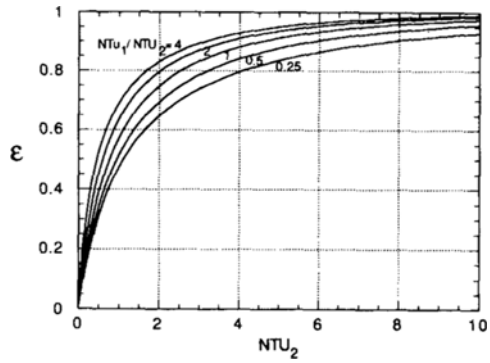

Fig. 7 ε as a function of NTU_1 and NTU_1/NTU_2
$C_1/C_3=0.4$, $C_2/C_3=0.8$, $\theta_2(1)=1$

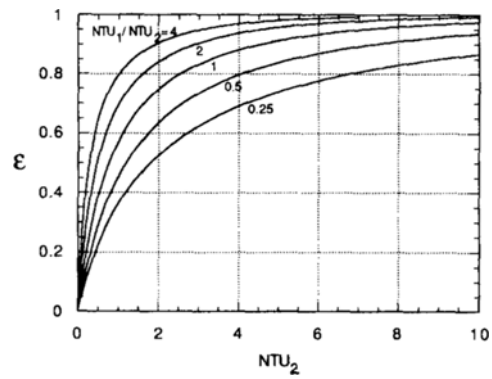

Fig. 8 ε as a function of NTU_1 and NTU_1/NTU_2
$C_1/C_3=0.8$, $C_2/C_3=0.4$, $\theta_2(1)=1$

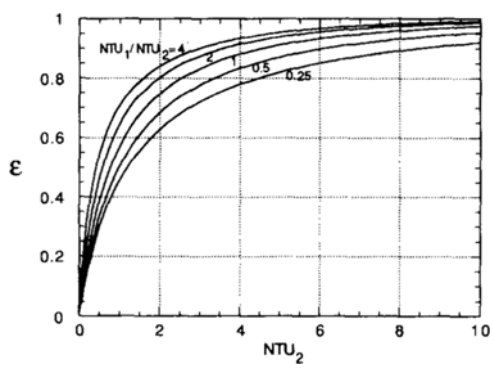

Fig. 9 ε as a function of NTU_1 and NTU_1/NTU_2
$C_1/C_3=0.4$, $C_2/C_3=0.8$, $\theta_2(1)=0.8$

$$\frac{1-\theta_1(0)}{1-(\theta_1(0))_{\min}} \approx \frac{\theta_2(1)-\theta_2(0)}{\theta_2(1)-(\theta_2(0))_{\min}} \approx \varepsilon \tag{22}$$

Equation (22) is exactly true from its definition when the effectiveness is close to 1 or the flow situation is balanced. However, the error of Eq.

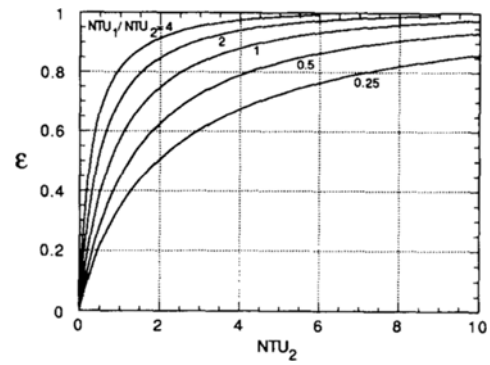

Fig. 10 ε as a function of NTU_1 and NTU_1/NTU_2
$C_1/C_3=0.8$, $C_2/C_3=0.4$, $\theta_2(1)=0.8$

(22) becomes large as the effectiveness decreases and the flow is extremely unbalanced. Since the triple-passage heat exchangers have been used only in cryogenic systems requiring very high effectiveness, Eq. (22) seems to be good enough for most of the cycle analysis. Quantitatively, it was confirmed from the numerical data sets that the relative error was less than 1% for the effectiveness of 0.90 or higher.

5. Summary and Conclusions

This work focused on developing a simple and accurate method to calculate the three exit temperatures at the triple-passage counterflow heat exchangers, for given inlet temperatures, capacity rates, heat transfer coefficients and heat transfer areas. The method thus developed can be summarized as the following procedures;

(1) nondimensionalize the inlet temperatures and the other parameters,

(2) calculate the the maximum or the minimum values of the exit temperatures by the analytical expressions,

(3) estimate "one" effectiveness, ε, from the listed graphs and proper interpolation,

(4) calculate the actual exit temperatures from their maximum or minimum values and the effectiveness.

The method was proven to be satisfactorily accurate for the practical design values of the parameters.

The most valuable contribution of the method

is that the calculation of the maximum heat transfer rates for very large NTU's was made possible with very simple steps. The maximum values are important not only in estimating the real heat transfer rate via the effectiveness, but also in indicating the thermodynamic limits in the cycle analysis or design. In this sense, the method is expected to play an important role in the design of the many contemporary cryogenic refrigeration and liquefaction systems.

Acknowledgement

This work is supported by the Korea Science and Engineering Foundation under grant No. 913-0901-013-2.

References

Aoki, K., Doi, Y., Kondo, Y, Shintomi, T., Makida, Y., Hashimoto, O., Kitami, T., Miyachi, T., Nagae, T. and Sekimoto, M., 1992, "Performance of Cryogenic Systems for a Large Superconducting Spectrometer Magnet," Advances in Cryogenic Engineering, Vol. 37, Part A, pp. 691 ~698.

Asakura, H., Kato, D., Saji, N. and Ohya, H., 1992, "80 K Centrifugal Compressor for Helium Refrigeration System," Advances in Cryogenic Engineering, Vol. 37, Part B, pp. 787~794.

Brindza, P., Chronis, W. and Rode, C., 1988, "CEBAF's Cryogenic System," Advances in Cryogenic Engineering, Vol. 33, pp. 623~630.

Chang, H.-M., Lee, T. I., Baik, J.H. and Cho, Y.-H., 1993, "A Study on the Cooling Systems of Superconducting Magnets for Medical Imaging," KOSEF Final Report No. 913-0901-013-2.

Clausen, J., Patzelt, A., Stephan, A. and Wanner, M., 1990, "The Linde-Turborefrigerator for MR-Tomographs," Advances in Cryogenic Engineering, Vol. 35, Part B, pp. 949~955.

Dauvergne, J.P., Firth, M., Juillerat, A., Lebrun, P. and Rieubland, J.M., 1990, "Helium Cryogenics at the LEP Experimental Areas," Advances in Cryogenic Engineering, Vol. 35, Part B, pp. 901~900.

Ganni, V., Moor, R. and Winn, P., 1986, "Capacity Upgrade of the Exell Helium Liquefier Plant by the Adding a Wet Engine," Advances in Cryogenic Engineering, Vol. 31, pp. 699~707.

Kays, W.M. and London, A.L., 1984, "Compact Heat Exchangers," 3rd ed., McGraw-Hill, New York, pp. 19~24.

Slack, D.S., Nelson, R.L. and Chronis, W.C., 1986, "Cryogenic Systems for the Mirror Fusion Test Facility," Advances in Cryogenic Engineering, Vol. 31, pp. 583~594.

Timmerhaus, K.D. and Flynn, T.M., 1989, "Cryogenic Process Engineering," Plenum Press, New York, pp. 261~266.

Tsuchiya, K., Ohuchi, N., Terashima, A. and Shinkai, K., 1990, "Cryogenic System of the Superconducting Insertion Quadrupole Magnets for Tristan Main Ring," Advances in Cryogenic Engineering, Vol. 35, Part B, PP. 941~948.

Tsuchiya, K., Ohuchi, N., Morita, Y., Sugahara, R., Kabe, A., Endo, K., Kawamura, S. and Matsumoto, K., 1992, "Helium Cryogenic Systems for the Superconducting Insertion Quadrupole Magnets of the Tristan Storage Ring," Advances in Cryogenic Engineering, Vol. 37, Part A, pp. 667~674.

Yamamoto, J., Mito, T., Motojima, O., Asami, T., Ebisu, H. and Otani, T., 1990, "Feasibility Study of Cooling System of New Superconducting Large Helium Fusion Reactor," Advances in Cryogenic Engineering, Vol. 35, Part B, pp. 967 ~974.

Yanagi, H., Yaguchi, H., Yabana, T., Fujima, K., Ino, N. and Yasuda, A., 1992, "The Planning of a Low Temperature Purifier for Super-GM Helium Refrigeration Plant," Advances in Cryogenic Engineering, Vol. 37, Part A, pp. 739 ~746.

Ziegler, B. and Quack, H., 1992, "Helium Refrigeration at 40 Percent Efficiency ?," Advances in Cryogenic Engineering, Vol. 34, Part A, pp. 645~951.